Journal of Geophysical Research: Space Physics

RESEARCH ARTICLE
10.1029/2018JA026073

Key Points:
- A model of artificial plasma layers created by the Arecibo HF facility is presented
- It shows that Langmuir turbulence due to the HF heating can accelerate part of the ambient photoelectrons to ionize the air
- The present model results are in quantitative agreement with the experiments of Bernhardt et al. (2017)

Correspondence to:
B. Eliasson,
bengt.eliasson@strath.ac.uk

Citation:
Eliasson, B., Milikh, G. M., Liu, T. C., Shao, X., & Papadopoulos, K. (2018). Simulations of the generation of energetic electrons and the formation of descending artificial plasma layers during HF heating at Arecibo. *Journal of Geophysical Research: Space Physics*, *123*, 10,301–10,309. https://doi.org/10.1029/2018JA026073

Received 7 SEP 2018
Accepted 18 NOV 2018
Accepted article online 8 DEC 2018
Published online 21 DEC 2018

Simulations of the Generation of Energetic Electrons and the Formation of Descending Artificial Plasma Layers During HF Heating at Arecibo

B. Eliasson[1,2], G. M. Milikh[2], T. C. Liu[2], X. Shao[2], and K. Papadopoulos[2]

[1]SUPA, Physics Department, University of Strathclyde, Glasgow, UK, [2]Departments of Physics and Astronomy, University of Maryland, College Park, MD, USA

Abstract High-frequency (HF)-induced descending artificial plasma layers (DAPLs) are artificially ionized plasma layers with plasma density in excess of that of the F_2 peak. They were discovered during HF heating experiments at the High-Frequency Active Auroral Research Program where they descended up to 70 km from the initial O mode wave reflection height. The DAPLs were attributed to the ionization of the neutral gas by high-energy electrons accelerated by the artificial ionospheric turbulence. Recently, DAPL formation was reported during the HF heating experiment at Arecibo (Bernhardt et al., 2017, https://ies2017.bc.edu/). This result was unexpected since Arecibo has the effective radiated power 4–5 times lower than that at High-Frequency Active Auroral Research Program, and since the experiment at Arecibo also has an unfavorable geometry, where the HF beam is directed vertically while the inclination of the geomagnetic field is 43.5°, allowing the fast electrons to escape the volume where their interaction with the artificial plasma turbulence occurs. However, the presence of photoelectrons due to the ultraviolet radiation from the Sun at the low latitude of Arecibo could magnify the flux of hot electrons. A model of artificial plasma layers created by the Arecibo HF facility is presented. It shows that Langmuir turbulence due to the HF heating can accelerate part of the ambient photoelectrons to energies above the ionization threshold of the neutral gas, leading to the formation of DAPLs. The present model results are in quantitative agreement with the experiments of Bernhardt et al. (2017).

Plain Language Summary A model of artificial plasma layers (APLs) created by the Arecibo high-frequency facility is presented. The APLs were recently detected at Arecibo. The model shows that Langmuir turbulence due to the high-frequency heating can accelerate part of the ambient photoelectrons to energies above the ionization threshold of the neutral gas, leading to the formation of APLs. The present model results are in quantitative agreement with the experiments.

1. Introduction

High-frequency (HF)-induced descending artificial plasma layers (DAPLs) are plasma layers driven by HF/plasma interactions with plasma density exceeding that of the F_2 peak. They were first observed during HF heating experiments at the High-Frequency Active Auroral Research Program (HAARP) (Pedersen et al., 2009, 2010). Mishin and Pedersen (2011) attributed the DAPLs to an ionization front created near the O mode critical layer caused by suprathermal electrons driven by strong Langmuir turbulence (SLT) acceleration in the ionospheric *F* region. The HF-driven ionization process, initiated near 220-km altitude subsequently descended and terminated at approximately 150-km altitude. The ionization/extinction process was repeated as long as the HAARP effective radiated power (ERP) exceeded a threshold value. Eliasson et al. (2012) using a complex simulation code demonstrated that the SLT acceleration depended on the presence of electrons with effective temperature in excess of 2–3 times the ambient electron temperature and attributed this to preheating/acceleration at the upper hybrid (UH) region, a few kilometers below. The connection of the DAPL and its relationship to the UH turbulence was later confirmed by subsequent observations by Mishin et al. (2016) that indicated that the most efficient DAPL generation takes place when the transmitted frequency is somewhat above multiple harmonics of the electron gyrofrequency and when the HF beam is directed toward the magnetic zenith to generate UH turbulence (Bernhardt et al., 2016; Sergeev et al., 2013). Numerical and analytical studies indicated that the efficiency of DAPL was dependent on whether the UH turbulence generated Druyvesteyn-type heating or high-energy tails processes that depended on whether the UH frequency was close to an electron cyclotron harmonic or not (Grach, 1999; Najmi et al.,

2017). However, the original observations by Pedersen et al. (2009) showed that DAPLs can be formed also when the HF wave is tuned below the local second electron cyclotron harmonic. Eliasson et al. (2015) presented a multiscale simulation model of the DAPL that includes SLT Langmuir acceleration of plasma electrons, the transport of energetic electrons to lower altitudes, and the ionization of neutral gas below the acceleration region by the energetic electrons and the buildup of plasma leading to reflection of the incident pump wave, that provided a closer to the early (Pedersen et al., 2009) and late DAPL observations (Mishin et al., 2016).

Recently, Bernhardt et al. (2017) reported the presence of DAPL during an HF heating experiment at Arecibo, where the DAPL descended about 20 km below the initial height of the O mode critical layer. This was unexpected since the Arecibo heater has an ERP 4–5 times lower than that at HAARP, and the magnetic geometry does not permit field aligned connection of the UH region to the SLT turbulence. The objective of this paper is to demonstrate that the well-known presence of photoelectrons (Carlson et al., 2016; Mishin et al., 2016; Perkins & Salpeter, 1965) can provide during daytime the ambient conditions for SLT acceleration even in the absence of the UH pre-acceleration required by HAARP.

We present below a multiscale simulation derived from our previous work (Eliasson et al., 2012, 2015) that addresses in detail the Arecibo DAPL observations. The model includes a full-wave simulation of the HF radio wave propagation, the excitation of SLT at the reflection point, a Fokker-Planck model of electron acceleration in the presence of ambient photoelectrons. The model is based on the realistic geometry of the vertical HF beam and oblique magnetic field. The resulting distribution of hot electrons is used in an ionization model for the major atmospheric particle species to estimate the plasma formation by the hot electrons. Finally, the model output is compared with the existing observations.

2. Theory

An ordinary (O) mode polarized radio wave injected into the overhead ionosphere excites SLT near the reflection point of the O mode wave when its amplitude exceeds the threshold for the oscillating two-stream instability, leading to spiky Langmuir oscillations trapped in ion density cavities (Rowland et al., 1981). Initially, the turbulence is primarily along the oscillatory electric field directed along the magnetic field lines, but later two-dimensional collapse may take place (Rowland et al., 1981; Russell et al., 1988). For simplicity we are using a one-dimensional full-wave model (discussed below) to estimate the wave packets created in the SLT. If the transit time of an electron is smaller than the wave period of the Langmuir wave as it traverses a localized wave packet, the electron feels a DC field and is efficiently accelerated or decelerated by the Langmuir wave. The process leads to a diffusion of the electron distribution function in velocity space that can be described by a Fokker-Planck equation. The diffusion coefficient is significantly large only if the field-aligned velocity of the electron exceeds satisfies the conditions $v > L/\omega_{pe}$, where L is the scale size of the soliton/cavity pair of the SLT and ω_{pe} the plasma frequency, and hence, for Maxwell-distributed electrons there is only small fraction of the electrons in the high-velocity tail distribution function that is efficiently accelerated by the SLT.

However, high-energy photoelectrons are produced in the Earth's ionosphere by photoionization of the neutral gas by the solar ultraviolet radiation. The excess photon energy transforms into a typical kinetic energy greater than 2 eV of the newly born photoelectrons, and these photoelectrons can be efficiently accelerated by the SLT. The photoelectron intensity F_ε peaks at an altitude of about 200 km, where its energy distribution turns out to be close to a shifted Maxwellian (interpolated from Figures 3.2.2 and 3.2.3 of Rees, 1989),

$$F_\varepsilon\left(\mathrm{cm}^{-2}\cdot\mathrm{s}^{-1}\cdot\mathrm{eV}^{-1}\right) = (1-2)\times 10^9 \exp\left[-m_e(v-v_0)^2/2T_{ph}\right] \quad (1)$$

with the peak velocity v_0 corresponding to a kinetic energy of about 3 eV, and the temperature T_{ph} = 4–6 eV. The factor $(1-2)$ corresponds to (solar minimum − maximum). The number density of the photoelectrons is obtained from

$$N_{ph} = \int F_\varepsilon/\mathrm{v}(\varepsilon)\,\mathrm{d}\,\varepsilon \quad (2)$$

Evaluating equation (2) with T_{ph} = 6 and using photoelectron intensity for the solar minimum and maximum (Rees, 1989) gives the corresponding number densities N_{ph} = 60 and 100 cm^{-3}, respectively. For the Arecibo

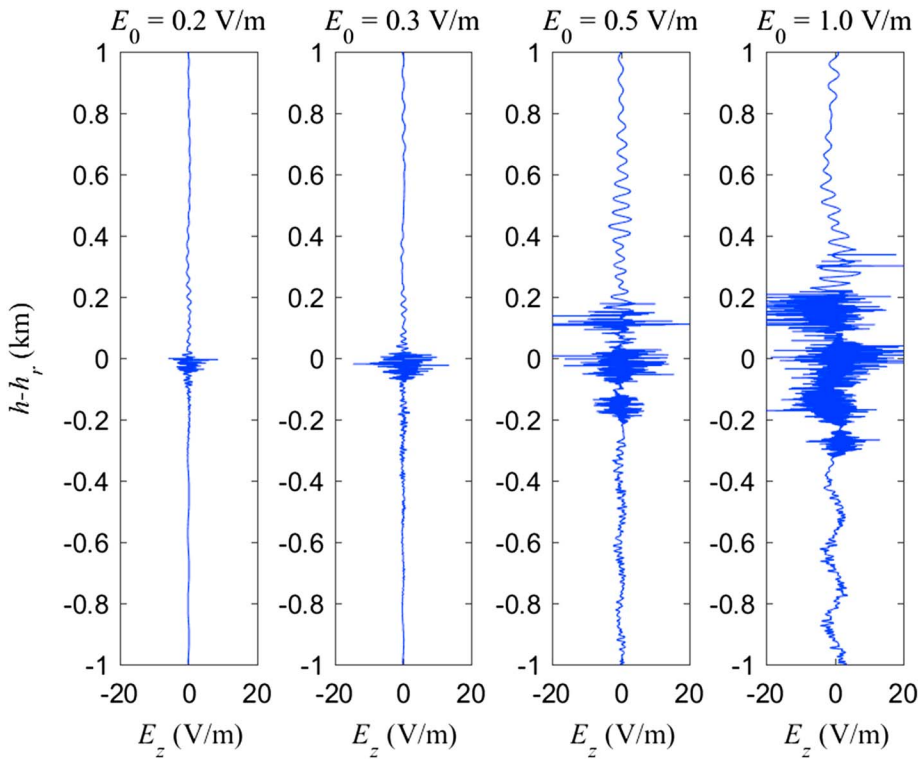

Figure 1. Turbulent electric fields vs. altitude $h - h_r$ calculated for injected O mode waves at amplitudes E_0 = 0.2, 0.3, 0.5, and 1.0 V/m. Here h_r is the reflection height of the O mode wave.

experiment (Bernhardt et al., 2017) the total electron number density N_e is found at the reflection point of the O mode wave by using the relation for the plasma frequency $f_{pe}(kHz) = 9\sqrt{N_e}$, where N_e is given in per cubic centimeters. The transmitted frequency 5,100 kHz gives $N_e \approx 3.2 \times 10^5$ cm^{-3}, and thus, the fraction of photoelectrons is $n_{ph} = N_{ph}/N_e \simeq (2 - 3) \times 10^{-4}$.

2.1. The Model Output

A set of simulations are carried out with a one-dimensional full-wave code (Eliasson et al., 2012, 2015), where an O mode wave with given amplitude is injected at the bottom of the simulation box and is allowed to propagate to the critical layer where it excites Langmuir turbulence. Details of the simulation model is given in Eliasson (2013). The ionospheric plasma profile is assumed to be on the form $N_e = N_{e0}\exp\left(-(z - z_0)^2/L_i^2\right)$ with $N_{e0} = 5.2 \times 10^5$ cm^{-3}, L_i = 63.25 km, and $z_0 = z_r$ + 44 km with z_r being the O mode reflection height. The geomagnetic field $B = 3.38 \times 10^{-5}$ T is tilted 43.5° to the normal. Using the *nonuniform nested grid method* (Eliasson, 2013), the simulations are done on a simulation box extending from $z = z_r - 78$ km to $z_r + 22$ km with a uniform grid size of 4 m to resolve the electromagnetic wave, and a finer, nested 2-cm grid is used locally in a 4-km-wide region $z = z_r - 3.5$ km to $z_r + 0.5$ km to resolve the small-scale electrostatic turbulence. This relaxes the stability condition on the time-step due to the electromagnetic wave, while simultaneously resolving the small-scale turbulence.

Figure 1 shows the turbulent HF electric fields versus altitude at t = 10 ms for injected O mode waves with the amplitudes E_0 = 0.2, 0.3, 0.5, and 1.0 V/m. The size of the turbulent region and the amplitude of the electrostatic waves increase with increasing amplitude of the pump wave. The lowest amplitude E_0 = 0.2 V/m serves as a threshold for the ionospheric turbulence, with no significant turbulence developing for $E_0 < 0.2$ V/m. Electromagnetic waves in the Z mode branch are seen to propagate at $h > h_r$. For the chosen plasma parameters, these Z mode waves propagate to the cutoff point of the Z mode wave at $h - h_r \approx 9$ km where they are reflected. When the converted Z mode waves are allowed to propagate over the F_2 peak to the conjugate point of the ionosphere, they may excite topside Langmuir turbulence (Eliasson, 2008) as observed in

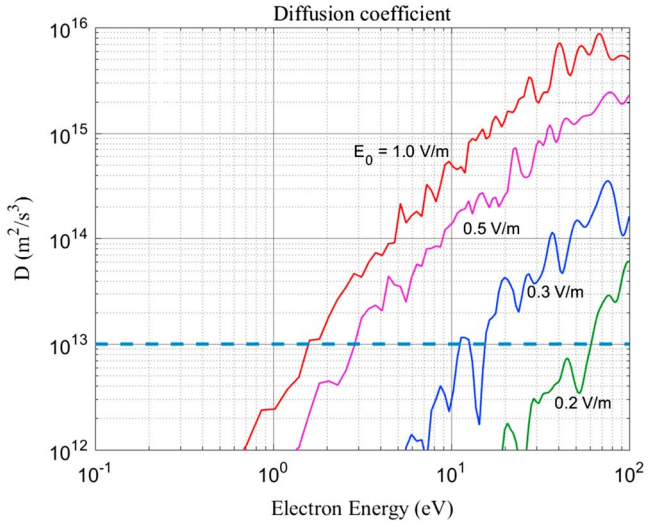

Figure 2. Diffusion coefficients calculated from the turbulent wave spectra of the electrostatic waves in Figure 1 for different values of injected O mode amplitude E_0. Efficient diffusion takes place for $D \gtrsim 10^{13}$ m^2/s^3 (dashed line).

experiments at Arecibo (Ganguly & Gordon, 1983) and European Incoherent Scatter Scientific Association (EISCAT) (Isham et al., 1990, 1999).

The small-scale Langmuir turbulence accelerate the electrons resonantly, leading to electron diffusion in velocity space. This process can be described by a Fokker-Planck equation (Eliasson et al., 2012; Sagdeev & Galeev, 1969)

$$\frac{\partial F}{\partial t} + v\frac{\partial F}{\partial z} = \frac{\partial}{\partial v} D(v) \frac{\partial F}{\partial v} \tag{3}$$

In SI units, the diffusion coefficient (m^2/s^3) is given by

$$D(v) = \frac{\pi e^2}{m_e^2} \frac{W_k\left(\omega, \frac{\omega}{v}\right)}{|v|} \tag{4}$$

where $W_k(\omega, k) = \Delta E^2/\Delta k$ (V^2/m) is the spectral energy density of the electric field per wavenumber Δk and ΔE^2 is the differential squared electric field.

We are here primarily interested in the ionization processes below the interaction region due to electrons that have streamed along the magnetic field lines through the turbulent region. We do not investigate in detail the space dependence of the diffusion coefficient within the turbulent region, but instead use an "averaged" diffusion coefficient based on the total spectrum of waves. While the turbulent wave spectrum is in general multidimensional (Grach, 1999; Ivanov et al., 1976; Vedenov et al., 1961), we have for simplicity used the one-dimensional Fokker-Planck model (3), consistent with our one-dimensional full-wave model. The diffusion coefficients corresponding to the turbulent electric fields in Figure 1 are shown in Figure 2. Low-energy electrons with energies below a few electron volts are only weakly accelerated by the turbulence. Electrons having energies of ~10 eV are efficiently accelerated for pump amplitudes $E_0 > 0.3$ V/m. In the Fokker-Planck simulations, a sum of Maxwellian electrons of temperature T_e = 2000 K and photoelectrons are injected at the boundaries, and the distribution function is broadened by the turbulence as the electrons traverse the turbulent region. When the electrons reach the opposite boundary, they are allowed to propagate over the boundary to be absorbed. The system reaches steady state approximately on a timescale when a low-energy electron with a speed equal to the ambient thermal speed $v_{te} = \sqrt{T_e/m_e} \sim 2\times10^5 m/s$ has traversed the turbulent region a few hundred meters wide. The Fokker-Planck simulations are run for 2 ms to ensure that steady state solutions have been achieved, after which the simulations are stopped and the resulting electron distribution functions are recorded.

Figure 3 shows the electron energy distribution function $f_e(\varepsilon)$ of the accelerated electrons, and the fraction of the population above a given energy, $n_e^{\rm hot}(\varepsilon) = \int_\varepsilon^\infty f_e(\varepsilon)d\varepsilon$. In the Fokker-Planck simulations, the fraction of

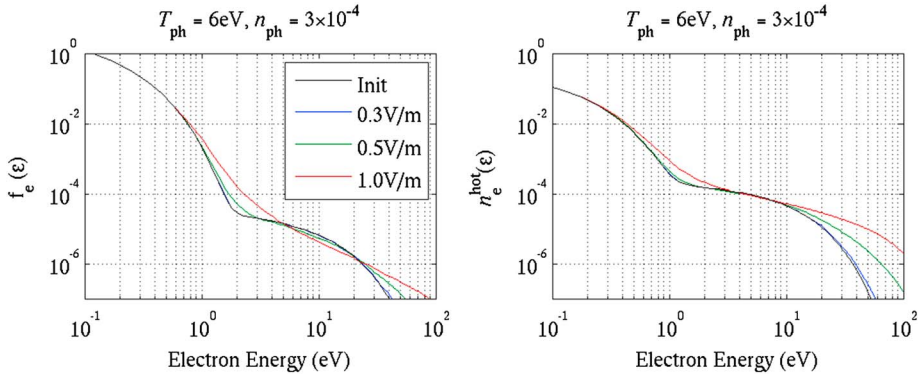

Figure 3. (left) The electron energy distribution $f_e(\varepsilon)$ and (right) the fraction of the population above the given energy $n_e^{\rm hot}(\varepsilon)$ for the initial ambient electron distribution ("Init") and for injected O mode amplitudes E_0 = 0.3, 0.5 and 1 V/m. The fraction of photoelectrons is $n_{ph} = 3 \times 10^{-4}$.

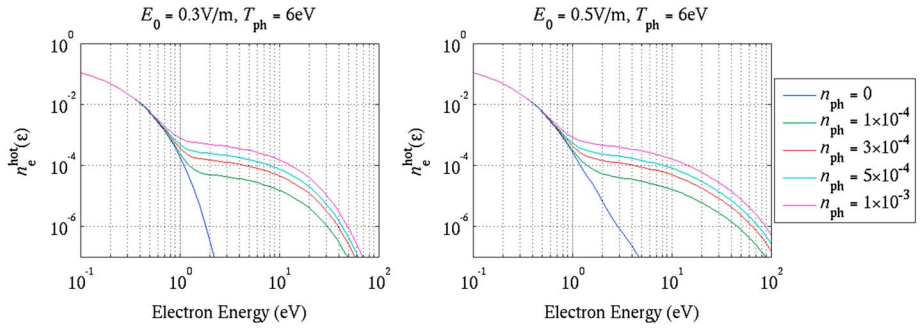

Figure 4. Fraction of the population above the given energy of hot electrons versus their kinetic energy computed for O mode wave injections at E_0 = 0.3 eV (left) and 0.5 eV (right). The blue line corresponds to the absence of photoelectrons, while the other lines correspond to the fraction of photoelectrons $n_{ph} = 10^{-4}$, 3×10^{-4}, 5×10^{-4}, and 10^{-3}.

photoelectrons injected at the boundaries is taken as $n_{ph} = 3 \times 10^{-4}$, and the diffusion coefficients were calculated using data from full-wave simulations with the injected O mode wave amplitudes E_0 = 0.3, 0.5 and 1 V/m. Figure 3 reveals that the high-energy tails above 15 eV of the accelerated electron population increases significantly with an increase of the pump amplitude E_0, and where E_0 = 0.3 V/m is too weak to significantly accelerate electrons.

In fact, the latter curve only slightly differs from the ambient photoelectron distribution shown by the black curve.

Figure 4 shows the fraction of hot electrons above a given energy for the cases where the injected O mode waves have the amplitudes E_0 = 0.3 and 0.5 V/m. The blue lines correspond to the acceleration of the thermal electrons in absence of photoelectrons, while the rest of the lines show results of the computations with the fractions of photoelectrons $n_{ph} = 10^{-4}$, 3×10^{-4}, 5×10^{-4}, and 10^{-3}, and with $v_0 = 1.03 \times 10^8$ cm/s and T_{ph} = 6 eV. Figure 4 reveals that adding the photoelectrons to the bulk of thermal electrons significantly increases the population of the electrons having the energy more than 15 eV, which can ionize the neutral atoms and molecules. The high-energy tail occurs due to the acceleration of the photoelectrons by the artificial plasma turbulence. Note that as shown in Figure 4 the HF electric field $E_0 < 0.5$ V/m is insufficient to accelerate the bulk of electron to energy >15 eV required for the ionization. Since at Arecibo $E_0 < 0.5$ V/m, only photoelectrons can be accelerated to ionize the neutral gas. A set of simulations (not shown) have revealed that the model depends only weakly on the temperature of the photoelectrons: when the value of T_{ph} was increased from 4 to 6 eV the number of the hot electrons with the energy 20 eV increased by less than 20%.

2.2. Estimates of the Artificial Ionization

The fast electrons are streaming downward and upward along the geomagnetic field from the turbulent plasma layer. They produce an additional ionization below the initial turbulent layer, where the number density of the neutral species is high enough

$$\Delta n_e = k_{ion} N_e^{hot} \tau_e^{life} \tag{5}$$

Here N_e^{hot} is the number density of the hot electrons, $k_{ion} = \sum_j N_j \kappa_{ion}^j$ is the total ionization rate by electron impact where the summation was made over the three major atmospheric species in the *F* region, N_2, O, and O_2. For the atmospheric species *j*, the number density is N_j and the ionization rate coefficient is given by

$$\kappa_{ion}^j = \int_{I_j}^{\infty} \sigma_{ion}^j(\varepsilon) \varepsilon f_e(\varepsilon) \mathrm{d}\varepsilon / \int_{I_j}^{\infty} \sqrt{\varepsilon} f_e(\varepsilon) \mathrm{d}\varepsilon \tag{6}$$

where σ_{ion}^j is the ionization cross section for the *j*th neutral component and I_j its ionization potentials (Rees, 1989); numerical values for ionospheric conditions at height 180 km are given in Table 1 below. The lifetime of the thermal electrons due to electron-ion recombination is

Table 1
The Number Density N_j, Ionization Potential I_j, and Ionization Rate Coefficient κ^j_{ion} in Equation (6) for the Major Atmospheric Species at Height 180 km

Atmospheric species	Number density at 180 km (cm^{-3})	Ionization potential (eV)	Ionization rate coefficient (cm^{-3}/s)
N_2	3.3×10^9	15.58	2.1×10^{-8}
O	4.7×10^9	13.61	1.5×10^{-8}
O_2	1.3×10^8	12.1	1.6×10^{-8}

$$\tau_e^{life} = 2/(\alpha_{ei} n_e). \quad (7)$$

The factor 2 in equation (5) reflects the fact that the dominant role is played by the dissociative electron recombination with the molecular ions which fraction is about 0.5 according to International Reference Ionosphere 2012 in the region of interest around 200 km (Bilitza et al., 2014).

To estimate the mean free path l for the hot electrons, we assume that the main electron energy losses are due to the ionizing collisions with the neutrals

$$l = 1/\left(\Sigma_j N_j \sigma^j_{ion}\right) \quad (8)$$

For the sake of simplicity, we assume monoenergetic electrons with the energy 20 eV. Taking the ionization cross-sections from Rees (1989) and the concentration of the major neutral species from the Committee on Space Research International Reference Atmosphere (2012) atmospheric model, we find that at 200 km the mean free path along the geomagnetic field is l = 30 km, while its vertical component is l_z = 20 km.

3. Comparison With Experiment at Arecibo

The Arecibo Observatory is located in Puerto Rico at 18◦N, 65◦W, where the inclination of the geomagnetic field is 43.5◦. The observatory hosts the HF Facility which can transmit radio waves at two HF frequencies, 5.1 and 8.175 MHz. The former is of our major interest since the ionosphere at the current moderate solar activity is underdense for f = 8.175 MHz, making this frequency inefficient for the generation of fast electrons. The HF Facility radiates 600-kW power and has the antenna gain G = 22 dB at f = 5.1 MHz. The antenna radiates a circular beam vertically, with the half power angular width 8.5◦. Thus, at 200 km height the diameter of the HF heated spot is 44 km. The free space electric field at the altitude h can be estimated as $E_0(\mathrm{V/m}) = 7.75\sqrt{ERP(\mathrm{MW})}/h(\mathrm{km})$ where ERP is the effective radiated power. For the Arecibo experiment, ERP = 95 MW, thus at h = 200-km height the electric field amplitude is E_0 = 0.4 V/m.

The recent experiment by Bernhardt et al. (2017) confirmed that DAPLs can be induced by the HF Arecibo facility. Results adopted from this experiment are presented in Figure 5. It shows plasma line measurements made by the Arecibo incoherent scatter radar. Figure 5 reveals that the HF heating induced plasma turbulence near the 5.1-MHz reflection point at around 200 km, which is marked by arrow 1 in Figure 5. The turbulent layer in turn generated the flux of fast electrons streaming downward and upward along the

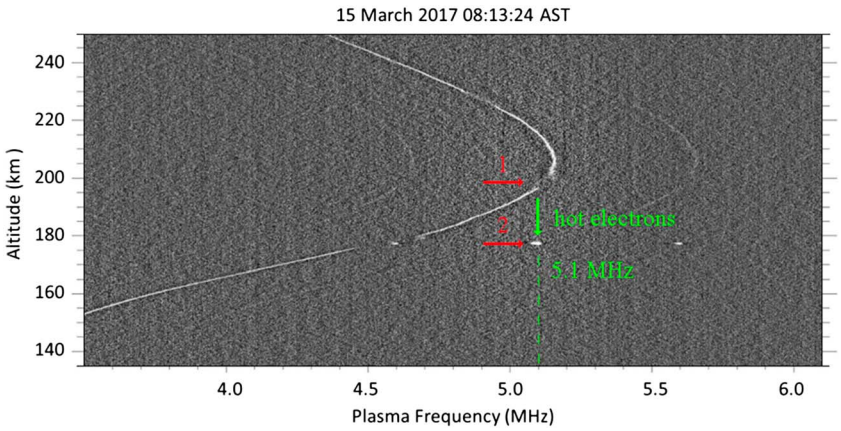

Figure 5. The electron plasma frequency versus altitude measured by the Arecibo incoherent scatter radar (adopted from Bernhardt et al., 2017). The turbulent layer produced near the 5.1-MHz wave reflection point is marked by the arrow 1. The secondary turbulent layer formed by the hot electrons 20 km below the original layer is marked by the arrow 2.

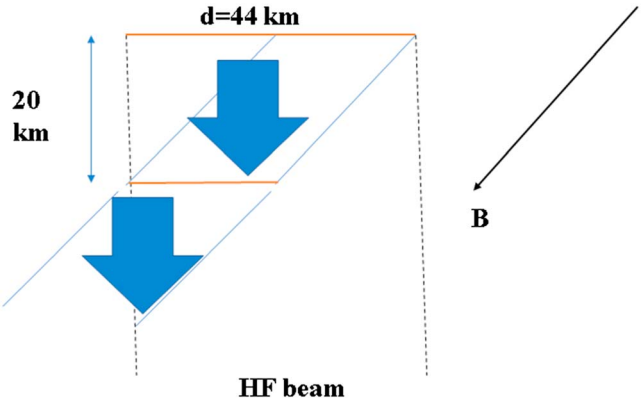

Figure 6. Schematic of the observed at Arecibo phenomenon. Two vertical dashed lines show the extent of the high-frequency (HF) beam. The hot electrons accelerated by the turbulent layer run downward along the magnetic field as shown by the fat arrows. The vertical component of the electron mean free path is shown by the two-head arrow on the left.

geomagnetic field. We focus on the effects caused by the downward propagation, since the upward moving electrons propagate into the rare ionosphere and do not produce a noticeable ionization. At about 20 km below the turbulent layer the fast electrons produce the plasma layer marked by the arrow 2 in Figure 5. The two dim spots at 4.6 and 5.6 MHz are caused by artifacts.

A schematic of the observed formation of a DAPL is shown in Figure 6. Two vertical dashed lines show the extent of the HF beam having a diameter d = 44 km. The HF beam is first reflected at 200 km, where it induces plasma turbulence, which in turn accelerates the ambient electrons. They stream downward along the magnetic field, obliquely to the vertical. The vertical component of the electron mean free path l_z = 20 km is indicated by the two-head arrow on the left. The hot electrons collide with the neutral particles and produce additional ionization, which is shown by the lower purple line. The incoming HF beam interacts with the newly produced plasma layer at 180 km. It is reflected and forms a thin turbulent plasma layer, which in turn generates hot electrons. Those electrons again run downward along the B field, but most of them are moving out of the HF beam. Therefore, unlike the experiments at HAARP (Mishin & Pedersen, 2011; Pedersen et al., 2010; Sergeev et al., 2013), where the HF beam was directed along the B field and maintained the DAPL propagation until it reached the lower ionosphere where the process was terminated by the electron-neutral collisions, in the discussed Arecibo experiment a DAPL propagating only one step is formed. Note that if the initial turbulent plasma layer would occur at a height below 200 km, the electron mean free path l_z would be smaller than 20 km and the DAPL could experience 2 or 3 shorter steps downward.

We estimate next the expected artificial plasma density produced by the fast electrons accelerated by the HF-induced turbulence using the results given in section 2.2. The number density of hot electrons is estimated in two steps. First, since the Arecibo 2017 experiment was made under normal solar conditions, we estimate the number density of photoelectrons as 80 cm^{-3} (see the text below equation (2)). It means that $N_e^{hot}/N_e \approx 3\times10^{-4}$ at 200 km where the plasma density is 3.2×10^5 cm^{-3}. Second, we run the Fokker-Planck simulation for the case with an injected O mode amplitude E_0 = 0.4 V/m and for the fraction of photoelectrons 3×10^{-4}. It is found that the number density of hot electrons with the energy higher than 20 eV is about 5 cm^{-3}.

The ionization rate at 180-km height is obtained by first evaluating equation (6) numerically for the three major atmospheric species N_2, O, and O_2, using the ionization cross sections and ionization potentials for the respective species given by Rees (1989). The results are shown in Table 1. The number density N_j for N_2, O, and O_2 was adopted from the Committee on Space Research International Reference Atmosphere (2012) atmospheric model for mean solar and geomagnetic activity. As a result, we find that $k_{ion}(z = 180\ km) = 200\ s^{-1}$. The lifetime of thermal electrons is estimated by using equation (7) in which recombination rate $\alpha_{ei} = 10^{-7} cm^{-3} \cdot s^{-1}$ and the electron density is 3.2×10^5 cm^{-3}, giving the lifetime $\tau_e^{life} =$ 60 s. Therefore, from equations (5)–(8) the artificial plasma density produced by the impact ionization of the hot electrons at 180 km altitude is about 0.6×10^5 cm^{-3}. According to the plasma line measurements shown in Figure 5 the electron plasma frequency at 180-km altitude is 4.6 MHz; that is, the ambient electron density at this height is 2.6×10^5 cm^{-3}. Therefore, the additional artificial ionization of about 0.6×10^5 cm^{-3} will result in full reflection of the O mode wave f = 5.1 MHz at 180-km altitude. It explains the observations made by Bernhardt et al. (2017) shown in Figure 5.

4. Conclusions

HF-induced DAPLs are artificially ionized plasma layers with plasma density in excess of that of the F_2 peak. They were first observed during HF heating experiments at HAARP and then explained in terms of an ionization front created near the O mode critical layer due to electrons energized by UH turbulence and injected to

HF excited SLT in the ionospheric *F* region. Recently, a DAPL was reported during the HF heating experiment at Arecibo (Bernhardt et al., 2017). This was unexpected since the Arecibo heater has an ERP 4–5 times lower than that at HAARP, and since the experiment has unfavorable geometry for UH turbulence and injection to SLT mode. However, the presence of photoelectrons produced by the solar ultraviolet radiation at the low latitude provides during day-time sufficient electron flux satisfying the SLT acceleration threshold, $>L/\omega_{pe}$, for ionization.

A model of DAPLs created by the Arecibo HF Facility is introduced. It is based on the modified multiscale simulation model of Eliasson et al. (2012), which includes a full-wave simulation of the HF radio wave and its excitation of SLT induced near the reflection point of the HF wave, and a Fokker-Planck model of electron acceleration with photoelectrons added to the ambient thermal electrons. The model is based on the realistic geometry of the vertical HF beam and oblique magnetic field. The resulting distribution of hot electrons are used in an ionization model for the major atmospheric particle species to estimate the plasma formation by the hot electrons.

The model shows that the hot electrons caused by the acceleration of the ambient photoelectrons by the artificial plasma turbulence, stream downward along the geomagnetic field and ionize the neutral gas when their energy exceeds about 15 eV. The ionization of the neutral gas increases the local plasma density thus the pump wave is reflected at a progressively lower altitude. This leads to formation of a new turbulent layer, consequently producing a set of DAPLs.

The present model results are in quantitative agreement with the Arecibo experiment. In fact, it explains why at Arecibo only one DAPL is formed below the initial turbulent layer, unlike multiple layers, which are formed at HAARP. The reason is that the Arecibo HF beam is vertical while the geomagnetic field is oblique; thus, the hot electrons streaming along the magnetic field can escape the volume where their interaction with the artificial plasma turbulence occurs.

Acknowledgments
This research is supported by AFOSR Grant F9550–14-1–0019. B.E. gratefully acknowledges support from the EPSRC (UK) Grant EP/M009386/1. Data used to produce figures and results for this paper are available at http://spp.astro.umd.edu/JGR_2018JA026073R/.

References

Bernhardt P. A., Briczinski, P. J. Siefring, C. L., Jackson-Booth, N., Nossa, E., Sulzer, M., et al. (2017). The international heating experiments (HEX) campaign at Arecibo. Paper presented at the *15th Ionospheric Effects Symposium (IES)*, Alexandria, VA. https://ies2017.bc.edu/

Bernhardt, P. A., Siefring, C. L., Briczinski, S. J., McCarrick, M., & Michell, R. G. (2016). Large ionospheric disturbances produced by the HAARP HF facility. *Radio Science*, *51*, 1081–1093. https://doi.org/10.1002/2015RS005883

Bilitza, D., Altadill, D., Zhang, Y., Mertens, C., Truhlik, V., Richards, P., et al. (2014). The International Reference Ionosphere 2012—A model of international collaboration. *Journal of Space Weather and Space Climate*, *4*, A07. https://doi.org/10.1051/swsc/2014004

Carlson, H. C., Djuth, F. T., & Zhang, L. D. (2016). Creating space plasma from the ground. *Journal of Geophysical Research: Space Physics*, *122*, 978–999. https://doi.org/10.1002/2016JA023380

Committee on Space Research International Reference Atmosphere (2012). COSPAR International Reference Atmosphere https://space-weather.usu.edu/cira/index, Chapter 1–3.

Eliasson, B. (2008). Full-scale simulation study of the generation of topside ionospheric turbulence using a generalized Zakharov model. *Geophysical Research Letters*, *35*, L11104. https://doi.org/10.1029/2008GL033866

Eliasson, B. (2013). Full-scale simulations of ionospheric Langmuir turbulence. *Modern Physics Letters B*, *27*(8), 1330005. https://doi.org/10.1142/S0217984913300056

Eliasson, B., Milikh, G., Shao, X., Mishin, E. V., & Papadopoulos, K. (2015). Incidence angle dependence of Langmuir turbulence and artificial ionospheric layers driven by high-power HF-heating. *Journal of Plasma Physics*, *81*(02), 415810201. https://doi.org/10.1017/S0022377814000968

Eliasson, B., Shao, X., Milikh, G., Mishin, E. V., & Papadopoulos, K. (2012). Numerical modeling of artificial ionospheric layers driven by high-power HF-heating. *Journal of Geophysical Research*, *117*, A10321. https://doi.org/10.1029/2012A018105

Ganguly, S., & Gordon, W. E. (1983). Heater enhanced topside plasma line. *Geophysical Research Letters*, *10*(10), 977–978. https://doi.org/10.1029/GL010i010p00977

Grach, S. M. (1999). On kinetic effects in the ionospheric *F*-region modified by powerful radio waves. *Radiophysics and Quantum Electronics*, *42*(7), 572–588. https://doi.org/10.1007/BF02677563.

Isham, B., Kofman, W., Hagfors, T., Nordling, J., Thidé, B., LaHoz, C., & Stubbe, P. (1990). New phenomena observed by EISCAT during an RF ionospheric modification experiment. *Radio Science*, *25*(3), 251–262. https://doi.org/10.1029/RS025i003p00251

Isham, B., Rietveld, M. T., Hagfors, T., La Hoz, C., Mishin, E., Kofman, W., et al. (1999). Aspect angle dependence of HF enhanced incoherent backscatter. *Advances in Space Research*, *24*(8), 1003–1006. https://doi.org/10.1016/S0273-1177(99)00555-4

Ivanov, A. A., Soboleva, T. K., & Yushmanov, P. N. (1976). Three-dimensional quasi-linear relaxation. *Soviet Physics - JETP*, *42*(6), 1027–1035.

Mishin, E., & Pedersen, T. (2011). Ionizing wave via high-power HF acceleration. *Geophysical Research Letters*, *38*, L01105. https://doi.org/10.1029/2010GL046045

Mishin, E., Watkins, B., Lehtinen, N., Eliasson, B., Pedersen, T., & Grach, S. (2016). Artificial ionospheric layers driven by high-frequency radiowaves: An assessment. *Journal of Geophysical Research: Space Physics*, *121*, 3497–3524. https://doi.org/10.1002/2015JA021823

Najmi, A., Eliasson, B., Shao, X., Milikh, G., Sharma, A. S., & Papadopoulos, K. (2017). Vlasov simulations of electron acceleration by radio frequency heating near the upper hybrid layer. *Physics of Plasmas*, *24*(10), 102904. https://doi.org/10.1063/1.4999768

Pedersen, T., Gustavsson, B., Mishin, E., Kendall, E., Mills, T., Carlson, H. C., & Snyder, A. L. (2010). Creation of artificial ionospheric layers using high-power HF waves. *Geophysical Research Letters*, *37*, L02106. https://doi.org/10.1029/2009GL041895

Pedersen, T., Gustavsson, B., Mishin, E., MacKenzie, E., Carlson, H. C., Starks, M., & Mills, T. (2009). Optical ring formation and ionization production in high-power HF heating experiments at HAARP. *Geophysical Research Letters*, *36*, L18107. https://doi.org/10.1029/2009GL040047

Perkins, F., & Salpeter, E. E. (1965). Enhancement of plasma density fluctuations by nonthermal electrons. *Physics Review*, *139*(1A), A55–A62. https://doi.org/10.1103/PhysRev.139.A55

Rees, M. H. (1989). *Physics and chemistry of the upper atmosphere*. New York: Cambridge University Press. https://doi.org/10.1017/CBO9780511573118

Rowland, H. L., Lyon, J. G., & Papadopoulos, K. (1981). Strong Langmuir turbulence in one and two dimensions. *Physical Review Letters*, *46*(5), 346–349. https://doi.org/10.1103/PhysRevLett.46.346

Russell, D., DuBois, D. F., & Rose, H. A. (1988). Nucleation in two-dimensional Langmuir turbulence. *Physical Review Letters*, *60*(7), 581–584. https://doi.org/10.1103/PhysRevLett.60.581

Sagdeev, R., & Galeev, A. (1969). *Nonlinear plasma theory*. New York: Benjamin.

Sergeev, E., Grach, S., Shindin, A., Mishin, E., Bernhardt, P., Briczinski, S., et al. (2013). Artificial ionospheric layers during pump frequency stepping near the 4th gyroharmonic at HAARP. *Physical Review Letters*, *110*(6), 065002. https://doi.org/10.1103/PhysRevLett.110.065002

Vedenov, A. A., Velikhov, E. P., & Sagdeev, R. Z. (1961). Nonlinear oscillations of rarified plasma. *Nuclear Fusion*, *1*(2), 82–100. https://doi.org/10.1088/0029-5515/1/2/003